AGU PUBLICATIONS

Geophysical Research Letters

RESEARCH LETTER
10.1002/2015GL063569

Key Points:
- Improved pattern scaling approaches are proposed and tested with CMIP5 models
- Skill improves when land-sea temperature contrast is considered
- Pattern scaling error is significantly smaller than the CMIP5 model spread

Supporting Information:
- Texts S1–S8, Figures S1–S5, and Tables S1 and S2

Correspondence to:
N. Herger,
nherger@student.ethz.ch

Citation:
Herger, N., B. M. Sanderson, and R. Knutti (2015), Improved pattern scaling approaches for the use in climate impact studies, *Geophys. Res. Lett.*, *42*, doi:10.1002/2015GL063569.

Received 19 FEB 2015
Accepted 2 APR 2015
Accepted article online 7 APR 2015

Improved pattern scaling approaches for the use in climate impact studies

Nadja Herger[1,2], Benjamin M. Sanderson[2], and Reto Knutti[1]

[1]Institute for Atmospheric and Climate Science, ETH Zürich, Zürich, Switzerland, [2]National Center for Atmospheric Research, Boulder, Colorado, USA

Abstract Pattern scaling is a simple way to produce climate projections beyond the scenarios run with expensive global climate models (GCMs). The simplest technique has known limitations and assumes that a spatial climate anomaly pattern obtained from a GCM can be scaled by the global mean temperature (GMT) anomaly. We propose alternatives and assess their skills and limitations. One approach which avoids scaling is to consider a period in a different scenario with the same GMT change. It is attractive as it provides patterns of any temporal resolution that are consistent across variables, and it does not distort variability. Second, we extend the traditional approach with a land-sea contrast term, which provides the largest improvements over the traditional technique. When interpolating between known bounding scenarios, the proposed methods significantly improve the accuracy of the pattern scaled scenario with little computational cost. The remaining errors are much smaller than the Coupled Model Intercomparison Project Phase 5 model spread.

1. Introduction

Anthropogenic warming of the climate system is well established and very likely to continue, but its magnitude and patterns of regional amplification are still uncertain because models are imperfect and because societal, technological, and economic developments are uncertain [*Intergovernmental Panel on Climate Change*, 2013]. To address the latter, scenarios were developed to represent alternative possibilities of how the future might unfold [*van Vuuren et al.*, 2011]. Four different Representative Concentration Pathways (RCPs) were introduced prior to the Fifth Assessment Report (AR5) of the Intergovernmental Panel on Climate Change (IPCC). The RCPs are an internally consistent set of pathways named after the radiative forcing they reach by 2100 [*Ebi et al.*, 2013; *Moss et al.*, 2010]. For impact studies in particular, four RCP scenarios are not sufficient to describe the full range of climate futures that might be experienced. However, running fully coupled climate models for many scenarios is impractical and computationally infeasible. Hence, computationally cheap statistical emulators for climate model output (among which pattern scaling is the most popular) are essential and used widely. Pattern scaling was first introduced by *Santer et al.* [1990] with the goal to create additional scenarios by scaling a (usually fixed) spatial response pattern to a forcing from a global climate model using a global mean temperature (GMT) anomaly obtained from a much simpler energy balance climate model [*Mitchell*, 2003]. Anomalies are traditionally considered relative to a preindustrial climate state. The basic assumptions of traditional pattern scaling have been shown to not always hold [e.g., *Tebaldi and Arblaster*, 2014]. In this study, we propose and assess alternatives and extensions to the simplest traditional pattern scaling technique and discuss the advantages and disadvantages associated with them. These approaches yield, in many cases, higher skill compared to the traditional one. Our skill metric is the mean squared error, for which we compare the field obtained by a global climate model (GCM) with a pattern scaled field.

2. Model and Data

For this study, GCMs from the Coupled Model Intercomparison Project Phase 5 (CMIP5) [*Taylor et al.*, 2012] were used. Most of our results are based on the following five GCMs: CESM1-CAM5, CCSM4, CSIRO-Mk3.6.0, HadGEM2-ES, and MIROC5. For each model the mean of three ensemble members per RCP was used to represent future changes. For some results the multimodel mean of 21 GCMs available in CMIP5 is used with one ensemble member per RCP and model (Table S1 in the supporting information). The data were regridded onto a T42 grid, and projections are made for the average over years 2080–2100 while the reference period is 1860–1880, which we consider to be a preindustrial period.

3. Methods

3.1. Traditional Pattern Scaling Approach

The simplest traditional pattern scaling approach approximates future changes by the product of a time-evolving GMT change and a pattern that varies spatially but is constant over time, scenario, and model characteristics [*Mitchell*, 2003] (see Text S1 in the supporting information). One underlying assumption of this approach is that responses to external forcing and internal variability are independent, implying that anthropogenic forcings do not modify the internal variability of the climate system [*Lopez et al.*, 2011]. So internal variability is assumed to be constant and is not scaled. This assumption might be true on decadal time scales and at smaller spatial scales. *Lopez et al.* [2013] found that it is unlikely that the external forcing will not modify the internal variability in a highly nonlinear system, especially on longer time scales. More elaborate pattern scaling techniques use a sum of several patterns that characterize the response to greenhouse gases and aerosols separately [e.g., *Frieler et al.*, 2012] where intermodel, interscenario, and interrun variability are taken into account.

Levy et al. [2013] found that traditional pattern scaling breaks down in the presence of significant aerosol forcing. Aerosol forcing is regionally variable and also influences precipitation. Generally, scaling of variables with high spatial variability has lower skill [*Tebaldi and Arblaster*, 2014]. Scaling is also less accurate for strong mitigation scenarios such as RCP2.6 [*May*, 2012]. The geographical distribution of warming changes as the climate system approaches equilibrium. *Manabe and Wetherald* [1980] explained this by the difference between the transient and the equilibrium response pattern, which is caused by the long adjustment time of the deep ocean. Moreover, scaling fails to capture changes in sea ice extent and snow cover [*Collins et al.*, 2013] which behave more like a boundary that moves poleward rather than a pattern that scales. Traditional pattern scaling only addresses the forced response, which implies that natural variability has to be treated separately [*Lopez et al.*, 2013]. Currently, it does not account for time-varying covariance between climate variables in the system [*Holden and Edwards*, 2010].

We first assess the skill of the traditional approach by quantifying the error in the emulated surface temperature change relative to the simulated RCP for 21 different models (e.g., by scaling RCP8.5 in the time period 2080–2100 to RCP4.5 and comparing this pattern to RCP4.5 obtained directly from the GCM). Figure S1 in the supporting information shows the error in the scaling of the multimodel patterns, but we observe a substantial intermodel spread in the error pattern for individual models. The general patterns showing the land-sea temperature contrast are consistent, but local errors of up to 0.5°C are seen in areas of deep water formation, sea ice, and in Central Asia. The biases could arise due to nonlinearities in model response to forcing, differing relative forcing contributions, and the fact that some scenarios are closer to equilibrium than others. To quantify the dominant effects, we apply a joint empirical orthogonal function (EOF) analysis to the four RCPs in 2080–2100 (with reference period 1860–1880, grid points weighted by their respective areas). All the RCPs were put together to form one large covariance matrix (where covariance is assessed in the domain defined by the gridded spatial points, and the four-member RCP ensemble). The mean of 21 models from the CMIP5 archive (one ensemble member per model and RCP, Table S1) was used.

The first EOF shown in Figure 1a explains the largest difference between the RCPs and simply reflects the larger global mean warming signal for the higher RCPs. This is effectively the pattern which is scaled in a traditional pattern scaling approach. This is confirmed in Figure 1d, where the first principal component (PC) is shown to be proportional to the GMT in the corresponding RCP. We see a stronger warming over land than over ocean in the first loading, partially explained by the larger heat capacity of the ocean which leads to a delayed response [*Joshi et al.*, 2008]. This differential warming between land and ocean regions is robust across models [*Fasullo*, 2010]. The reduced warming in the North Atlantic can be explained by the projected reduction of the Atlantic Meridional Overturning Circulation as the climate warms [*Weaver et al.*, 2012].

The second EOF (Figure 1b) explains the largest fraction of variance across the RCPs that is not captured in Figure 1a and represents the largest errors introduced by traditional pattern scaling. EOFs do not necessarily corresponded to specific processes, and we interpret this pattern as a combination of three main phenomena: (1) The land area warms up even more for the high RCPs, whereas some parts of the ocean surface are cooler than expected from the first EOF, owing to the different heat capacities of land and ocean. As a result of polar amplification from ice- and snow-albedo feedbacks, land areas in high northern latitudes show the strongest warming in the first mode, but the second loading shows that for higher forcing scenarios this effect is relatively less because some fraction of the snow and ice is already lost. Moreover, loading two gives a retarding of

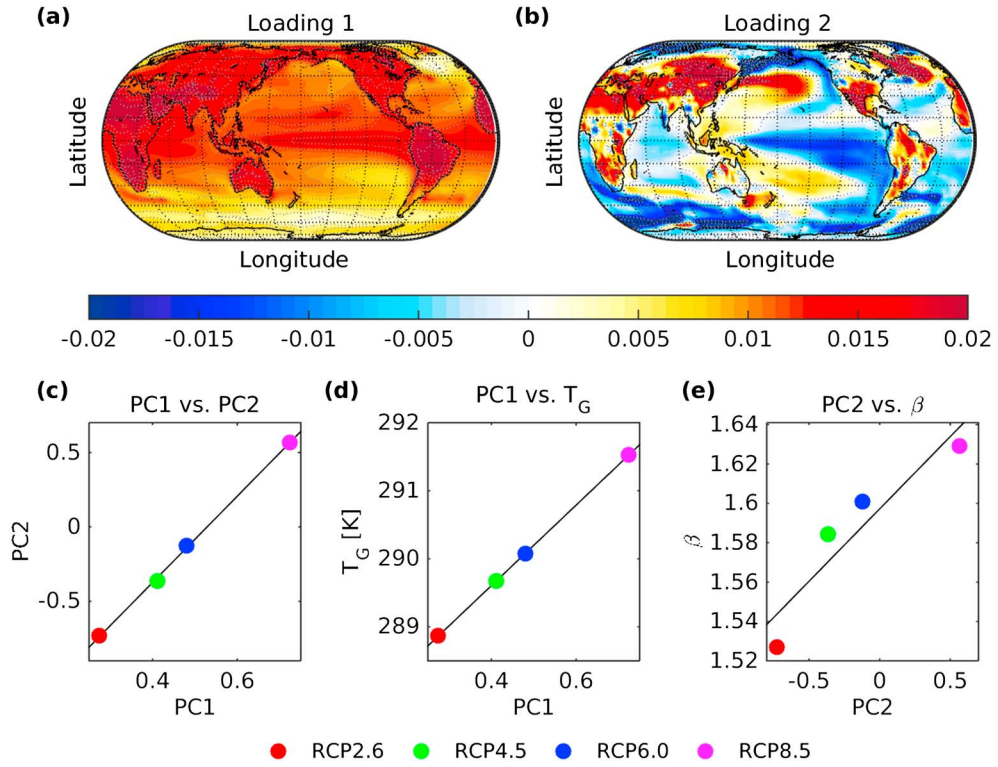

Figure 1. EOF analysis of the area-weighted temperature fields (2080–2100) of the four RCPs with reference period 1860–1880. The loadings of the (a) first and (b) second EOF are shown. (c) The first principal component (PC1) versus PC2. (d) PC1 plotted against the GMT, T_G, of the RCPs and (e) PC2 versus the land-sea temperature contrast (β in equation (S3) in the supporting information). Linear regressions were fitted to the four points. Twenty-one models from the CMIP5 archive with one ensemble member per scenario were used.

the warming, which may be a result of cold deep water upwelling. (2) The overall pattern resembles the Pacific Decadal Oscillation (PDO), which is a long-lived pattern of climate variability in the Pacific, with El-Niño-like features [*Zhang et al.*, 1997] in the tropical Pacific. The sea surface temperature in the North Pacific is strongly influenced by the PDO. However, using the PDO index for pattern scaling purposes was found to be difficult as models differ in their skill to represent the PDO correctly. This implies a large, model-dependent variability which projects onto this pattern. (3) An interesting pattern is observed in the North Atlantic, which shows a warming in that region, but the cause of it is unclear. It is model dependent and not consistent enough to be used as a predictor. A consistency analysis across the five models is shown in Figure S2.

The first and second PCs are almost perfectly correlated (Figure 1c), but they are not proportional. Accounting for some of the variance captured in the second loading can still increase the skill by accounting for any variables which are not proportional to global surface temperature change. The second EOF analysis suggests that the land-sea temperature contrast should be used as second predictor, as it is the largest feature and most consistent across models among those identified above. Figure 1e shows that the PCs of the second EOF scale well with the land-sea temperature contrast (see section 3.3).

Figure 1b suggests that errors are introduced in traditional pattern scaling because land and ocean regions warm at different rates, and these differences are influenced both by the amplitude and rate of warming. If a prediction over land is most relevant for impact studies then the simplest way to address this is a pattern scaling approach using global land temperature instead of GMT as a predictor. This approach turns out to have in almost all cases smaller mean squared errors, but only by a few percent (see Text S4). Hence, we focus on approaches with larger improvements in skill in the remainder of this study.

3.2. Time Shift Approach

To predict temperatures in RCP4.5 in 2080–2100 with the traditional approach, we can, for example, scale down RCP8.5 in 2080–2100 based on the GMT change. An alternative is to apply the "time shift" approach, which finds the time segment in RCP8.5 in which the average temperature matches the required global mean

surface temperature. Hence, no scaling is needed, and the time window is simply chosen appropriately, which makes the approach easy to apply. This approach has some important advantages: Consistency between multiple variables (e.g., physical relationship between temperature and precipitation) and correlation in space and time is fully preserved. The internal variability does not have to be scaled in magnitude and is consistent with the global temperature change. In addition, consistency is ensured even for quantities that do not scale (e.g., the edge of Arctic sea ice) to the degree that regional changes depend on global temperature and are adequately represented in the model. Finally, it is highly unlikely that the resulting pattern shows something completely nonphysical, because no scaling is required. However, this technique also has limitations. For example, it is impossible to use a time period from RCP2.6 to predict RCP8.5 in 2080–2100 because the RCP2.6 scenario never reaches the GMT of RCP8.5. This approach makes the assumption that the pattern at a given GMT change is independent of the rate of temperature change. On short time scales, this underlying assumption must be justified in a case by case basis. If the rate of change of forcing (or the nature of the forcing itself) differs significantly between the predicted time period and the predictor simulation, this could potentially introduce error into the approach. Nevertheless, those assumptions appear to be less problematic than those made by scaling patterns for fixed time periods (see section 4).

3.3. Approach With Multiple Predictors

If the traditional pattern scaling is primarily limited by its inability to represent nonlinear feedbacks, those could be resolved by a second-order (quadratic) term in GMT to better fit some nonlinearities in the system. This is a purely mathematically motivated approach, and we do not claim that those nonlinearities are expected to scale quadratically with GMT. We tested this idea but due to its lack of physical justification and bad performance for extrapolation, we only briefly discuss it in Text S6 of the supporting information.

A more physically motivated approach is the use of a second predictor representing the land-sea temperature contrast to account for some of the patterns which are ignored by traditional pattern scaling, as already suggested by *Joshi et al.* [2013]. They included the land-sea surface warming ratio $T_{\mathrm{land}}/T_{\mathrm{sea}}$ in addition to the transient climate response of the climate models to explain the intermodel variance between 22 GCMs from the CMIP3 archive. In contrast, we here do not aim to explain the variance between models but introduce a second predictor which increases the skill in creating new scenarios. With a second predictor, two scenarios are needed to calculate the scaling factors. This approach basically consists of two equations (one equation per RCP) with two unknowns (scaling factors), see Text S5 in the supporting information.

We define our land-sea contrast term, β, as a dimensionless factor which describes the differential warming of land and ocean and represents the component of land-sea contrast which is not explained by global mean warming. It is the land temperature deviation from the preindustrial state divided by the sea surface temperature anomaly. Figure 1e shows that there is a strong relationship between β and PC2.

In Figure S4b in Text S7, we present the smoothed temporal evolution of the multimodel mean β between 1966 and 2100 for the historical data and the four RCPs. Because we expect the land-sea temperature difference to be larger in a simulation with rapidly increasing forcing (where the land would be adjusting rapidly, but the ocean response would be delayed), we can interpret β as characterizing the system's disequilibrium. It turns out to be very sensitive to different properties of land and oceans. In the historical data we identify two large volcanic eruptions and the different character of each RCP is clearly reflected in the time series of β. The curve of RCP8.5 flattens out toward the end of the century as a constant growth rate is reached, and for RCP2.6 the overshoot is visible. This strongly suggests that β is related to the rate of warming and contains information which is independent of the absolute value of the warming, making it a promising second predictor.

4. Results and Discussion

The traditional pattern scaling, the time shift approach, and the bivariate approach with land-sea contrast were tested for all possible combinations of RCPs and discussed in this section. To illustrate our results we present error maps (pattern scaled surface temperature and precipitation fields minus fields obtained with GCMs) for the case of predicting RCP4.5 in 2080–2100 when RCP2.6 and RCP8.5 are known (Figure 2). Three different pattern scaling techniques were applied: Traditional pattern scaling (Figures 2a and 2d), time shift approach (Figures 2b and 2e), and the bivariate approach with the land-sea contrast as second predictor (Figures 2c and 2f). The largest errors in surface temperature are observed in the North Atlantic and the regions with substantial sea ice extent changes. The predicted land temperatures in Figures 2a and 2b are too high.

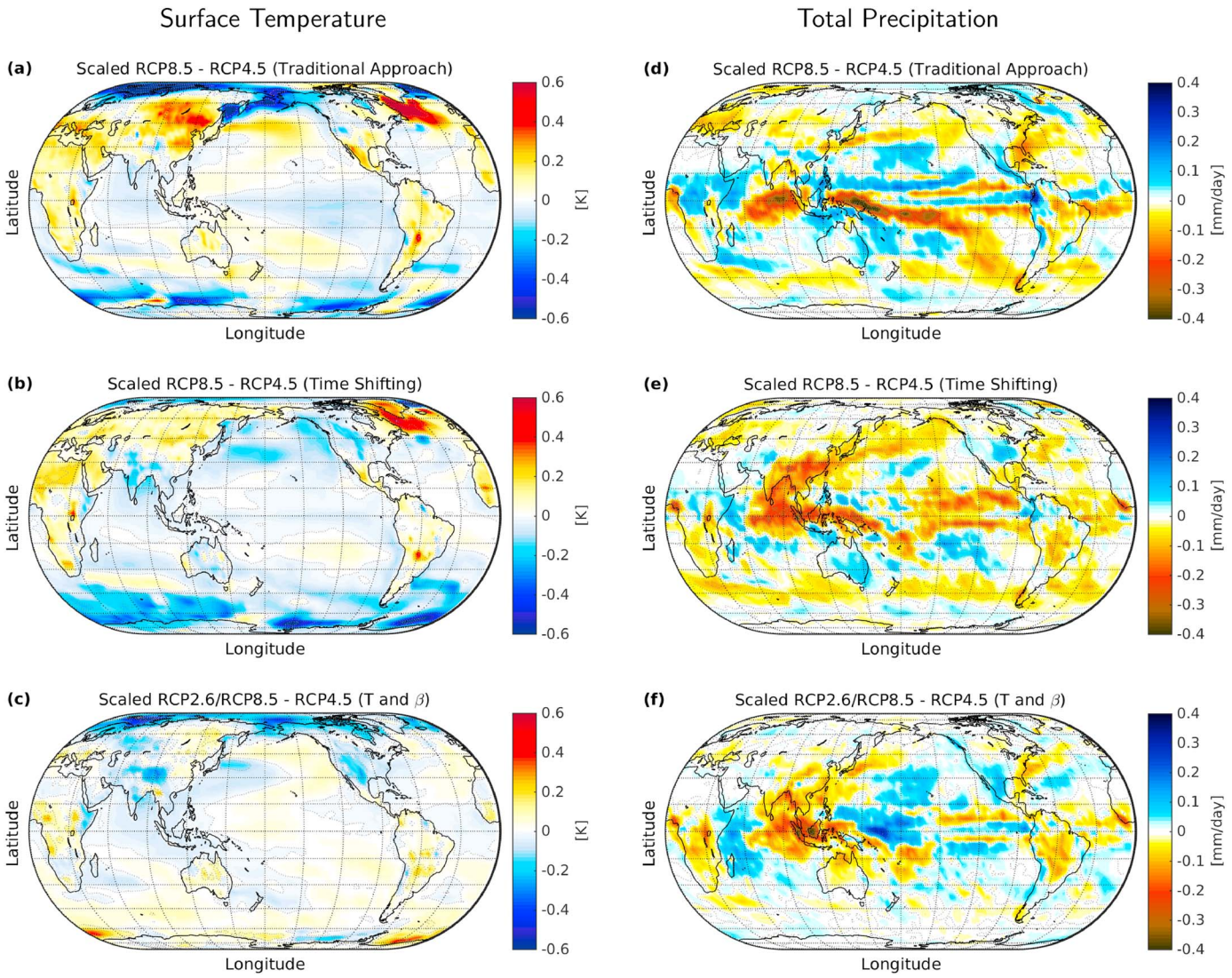

Figure 2. Error plots obtained with (a and d) the traditional pattern scaling approach, (b and e) the time shift approach, and (c and f) the bivariate approach with the land-sea contrast term. In all the cases, the multimodel mean of 21 GCMs is used and we assume that only RCP2.6 and RCP8.5 are known. RCP4.5 in 2080–2100 is predicted. The results are shown for surface temperature (Figures 2a–2c) and precipitation (Figures 2d–2f).

This is no longer the case in Figure 2c, where the land-sea temperature contrast is taken into account. The errors in the pattern scaled fields decrease from Figures 2a to 2c and from Figures 2d to 2f. For precipitation, the largest errors occur in the Intertropical Convergence Zone (ITCZ) and in the Indian Ocean. It suggests that a shift of the ITCZ cannot be well represented by pattern scaling.

We repeated this analysis for all the proposed pattern scaling approaches and possible RCP combinations. The result is summarized in Figure 3. The boxes represent the spread in error introduced by pattern scaling in five different GCMs. Brackets on top of the corresponding box indicate the number of failed pattern scaling approaches out of five. A pattern scaling approach was considered "failed" when the error in one model was more than 10 times larger than the average of the errors obtained with the other four models. The asterisks represent the results when the multimodel mean of 21 GCMs was used.

Error ratios (estimated at the grid box and combined in an area-weighted average) for scaling surface temperature (Figures 3a–3d) and precipitation (Figures 3e–3h) are shown. The ratio consists of the errors obtained through pattern scaling relative to the intermodel spread (five GCMs) in the prediction of the respective RCP, i.e., the mean squared errors (MSE) between pattern scaling and the true model and relative to the MSE between each combination of models. In contrast to errors introduced by the pattern scaling, the intermodel

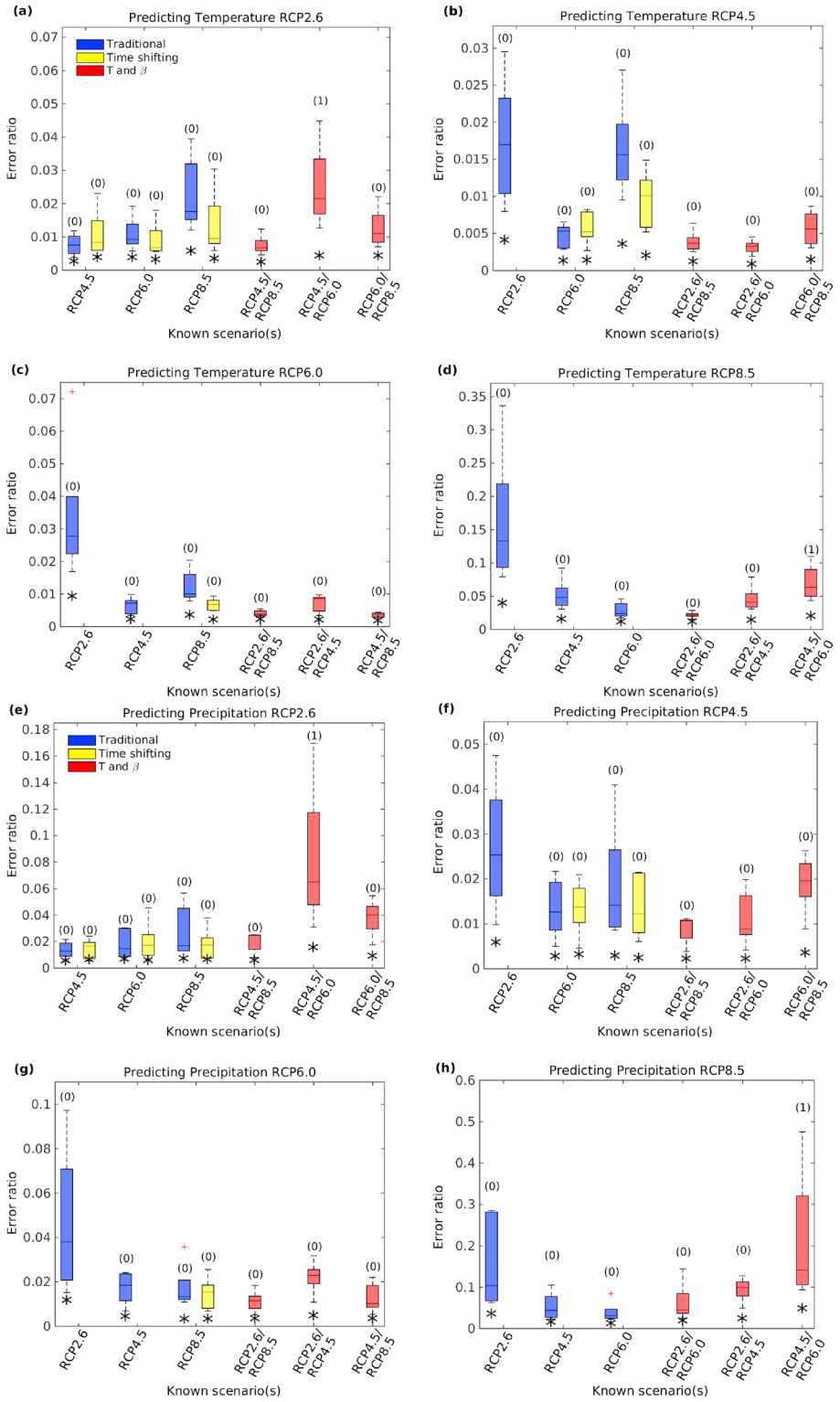

Figure 3. Comparison of the different pattern scaling approaches for (a–d) temperature and (e–h) precipitation. The RCPs in 2080–2100 were predicted using five GCMs (three ensemble members per model). The number of models, in which the pattern scaling approach failed (out of five) is shown in brackets above the corresponding box plot. The asterisks represent the results of scaling the multimodel mean (21 models with one ensemble member per RCP). Errors are expressed as ratios between the error introduced by pattern scaling approach and the mean intermodel spread.

spread should not be regarded as an error. The differences between the models are caused by differences in processes included or neglected and by internal variability. Ratios below 1 mean that the error introduced by pattern scaling is small compared to the intermodel spread. Smaller error ratios imply higher skill of the corresponding pattern scaling technique. We find in almost all cases that the errors introduced by pattern scaling are significantly smaller than the differences between GCMs (see also Figure S5).

4.1. Interpolation Versus Extrapolation

Interpolation (Figures 3b, 3c, 3f, and 3g) is found to have higher skill than extrapolation (Figures 3a, 3d, 3e, and 3h) for the two-predictor approach. Unsurprisingly, the traditional approach works best when the known scenario is close to the predicted one (see also Figure S1). For the bivariate prediction, the skill is highest when the known scenarios bound the predicted one. Additionally, the skill increases with larger difference between the two known scenarios when extrapolating. The time shift approach also works better when the known and predicted scenarios have similar radiative forcings. The derived time segment in the known RCP then lies closer to the predicted one, and less errors caused by different warming rates are introduced.

4.2. Robustness

The time shift method is robust in the sense that it is skillful and effective in most cases, provided that a time period with matching temperature is available. In contrast to the other techniques, no scaling is applied and all output fields are taken directly from existing simulations, making the patterns physically self-consistent (to the degree that the relevant processes are correctly represented in the GCM). It outperforms the traditional approach in most of the cases. In the other approaches, temperature and precipitation are scaled separately and physical relationships between multiple variables are not preserved. The approach with the land-sea contrast rarely shows unrealistic results when extrapolating and often outperforms the techniques with only one predictor.

4.3. Variability Scaling

Pattern scaling only applies to the externally forced climate response and not to the natural variability [*Collins et al.*, 2013]. The correct representation of internal variability is particularly important on small spatial scales and on short time scales [*Hawkins and Sutton*, 2009]. Depending on how many simulations are available and the interest of the end user, natural variability can be estimated separately and added to the scaled forced response [e.g., *Lopez et al.*, 2013]. Alternatively, variability can be estimated from long control simulations, but this assumes that variability does not change with external forcing. A recent paper by *Screen* [2014] showed a decrease in variability with increasing GMT, which is largest in middle and high latitudes. For extrapolation far into the future, it is essential to account for this change in variability. The time shift approach is the only method which preserves variability. The results for scaling the multimodel mean are shown as asterisks in Figure 3. It is evident that the error ratio is smaller when considering the multimodel mean, where the internal variability is significantly reduced. Nonetheless, the above mentioned advantages and drawbacks of the different pattern scaling approaches still hold.

4.4. Implications for the Experimental Design

Scenarios provide important climate projections to support a variety of research fields, such as adaptation, mitigation, and impacts. Because GCM simulations are computationally expensive, and other communities require many scenarios, our results should be considered in the process of the experimental design of scenarios. Figure 3 shows that the bivariate pattern scaling technique has highest skill if bounding scenarios exist. This finding could be exploited in future experimental design of scenarios. Skill decreases quickly for extrapolation.

5. Conclusions

In this present study we propose and test new methods to complement the traditional pattern scaling approach. The "time shift" approach finds a time segment with matching GMT from an already existing simulation to approximate a period in a desired scenario. The consistency between variables and the correlation in space and time is preserved, and internal variability does not require scaling. However, if climate patterns are a function of both the absolute value of global mean warming and the rate of warming, then those effects will not be represented in a time shift method. This might not be a problem when the desired and known time segments are close. On longer time scales, neglecting the scenario-dependent rate of warming might lead to decreased skill. However, for the scenarios tested, this is less problematic than scaling patterns for fixed time

periods as in the traditional approach. The approach can also only be used if a period of comparable GMT is available in an existing simulation.

As an alternative, we propose a bivariate pattern scaling method. We consider the ratio of land-sea temperature difference to global mean warming, motivated by the finding that the error fields from a traditional pattern scaling show that a portion of the land-sea contrast does not scale linearly with GMT. This contrast is effectively a proxy for the climate system's rate of change of warming. With the land-sea temperature contrast as a second predictor, the skill significantly exceeds that of the traditional one when the two known scenarios bound the predicted one and produces better or comparable results in extrapolation.

In all our analyses we applied the pattern scaling techniques to the mean signal and ignored the internal variability, which is assumed to be constant under traditional pattern scaling. However, recent studies show that this is not fully justified, as temperature variability in middle and high latitudes was found to decrease with increasing GMT [*Screen*, 2014; *Fischer and Knutti*, 2014]. Any study attempting to incorporate variability information into pattern scaled results would likely need to take these effects into account. We tested our approaches on a T42 grid and applied them to 20 year mean temperature and precipitation fields. Whether our approaches can deliver skillful information at decision relevant spatial and temporal scales need further investigations, but those limitations apply equally to GCM results without pattern scaling.

We find, in conclusion, that in most cases, the traditional approach with only GMT as a predictor can be significantly improved using the time shift approach (if possible) or a bivariate predictor using a component of land-sea temperature contrast in addition to GMT. Given a set of two bounding scenarios (in this case, RCP2.6 and RCP8.5), this study suggests that we can significantly increase the accuracy of the predicted response for forcing levels between these two values. Skill in predicting surface temperature and precipitation can be increased by a factor of up to 4 and 3, respectively. As an interpolant, the bivariate approach requires the end user to compute both land and ocean temperatures in a simple model, but our findings suggest that this small increase in complexity is worthwhile. The Model for the Assessment of Greenhouse-gas Induced Climate Change/ A Regional Climate Scenario Generator (MAGICC/SCENGEN) is an example of such a simple modeling tool [*Meinshausen et al.*, 2011].

The error introduced by pattern scaling is small (1–15% for temperature and 2–30% for precipitation) compared to the intermodel spread in the variable itself. The former is therefore largely insignificant relative to the large uncertainty in the predicted future by different models. The irreducible error defined as the spread between ensemble members is similar to one of the pattern scaling approaches (see Figure S5). The errors of pattern scaling for temperature and precipitation are larger than the irreducible one but almost an order of magnitude smaller than the CMIP5 model uncertainty. Impact modelers and other end users are interested in having a wide range of possible futures to assess risk. Our proposed pattern scaling techniques could potentially improve the mean state predictions for pattern scaled estimates of future climate change, allowing the simulation of a variety of future climate outcomes within two bounding scenarios at very low computational cost.

Acknowledgments

We acknowledge the World Climate Research Programme's Working Group on Coupled Modeling, which is responsible for CMIP, and we thank the climate modeling groups (listed in Table S1 of the supporting information of this paper) for producing and making available their model output. For CMIP the U.S. Department of Energy's Program for Climate Model Diagnosis and Intercomparison provides coordinating support and led development of software infrastructure in partnership with the Global Organization for Earth System Science Portals.

The Editor thanks two anonymous reviewers for their assistance in evaluating this paper.

References

Collins, M., et al. (2013), Long-term climate change: Projections, commitments and irreversibility, in *Climate Change 2013: The Physical Science Basis. Contribution of Working Group I to the Fifth Assessment Report of the Intergovernmental Panel on Climate Change*, edited by T. F. Stocker et al., pp. 1029–1136, Cambridge Univ. Press, Cambridge, U. K., and New York., doi:10.1017/CBO9781107415324.024.

Ebi, K. L., et al. (2013), A new scenario framework for climate change research: Background, process, and future directions, *Clim. Change*, *122*(3), 363–372, doi:10.1007/s10584-013-0912-3.

Fasullo, J. T. (2010), Robust land-ocean contrasts in energy and water cycle feedbacks, *J. Clim.*, *23*, 4677–4693, doi:10.1175/2010JCLI3451.1.

Fischer, E. M., and R. Knutti (2014), Impacts: Heated debate on cold weather, *Nat. Clim. Change*, *4*, 537–538, doi:10.1038/nclimate2286.

Frieler, K., M. Meinshausen, M. Mengel, N. Braun, and W. Hare (2012), A scaling approach to probabilistic assessment of regional climate change, *J. Clim.*, *25*(9), 3117–3144, doi:10.1175/JCLI-D-11-00199.1.

Hawkins, E., and R. Sutton (2009), The potential to narrow uncertainty in regional climate predictions, *Bull. Am. Meteorol. Soc.*, *90*(8), 1095–1107, doi:10.1175/2009BAMS2607.1.

Holden, P. B., and N. R. Edwards (2010), Dimensionally reduced emulation of an AOGCM for application to integrated assessment modelling, *Geophys. Res. Lett.*, *37*, L21707, doi:10.1029/2010GL045137.

Intergovernmental Panel on Climate Change (2013), *Climate Change 2013: The Physical Science Basis. Contribution of Working Group I to the Fifth Assessment Report of the Intergovernmental Panel on Climate Change*, edited by T. F. Stocker et al., 1535 pp., Cambridge Univ. Press, Cambridge, U. K., and New York, doi:10.1017/CBO9781107415324.

Joshi, M. M., J. M. Gregory, M. J. Webb, D. M. H. Sexton, and T. C. Johns (2008), Mechanisms for the land/sea warming contrast exhibited by simulations of climate change, *Clim. Dyn.*, *30*(5), 455–465, doi:10.1007/s00382-007-0306-1.

Joshi, M. M., A. G. Turner, and C. Hope (2013), The use of the land-sea warming contrast under climate change to improve impact metrics, *Clim. Change*, *117*(4), 951–960, doi:10.1007/s10584-013-0715-6.

Levy, H., II, L. W. Horowitz, M. D. Schwarzkopf, Y. Ming, J. -C. Golaz, V. Naik, and V. Ramaswamy (2013), The roles of aerosol direct and indirect effects in past and future climate change, *J. Geophys. Res.*, *118*, 4521–4532, doi:10.1002/jgrd.50192.

Lopez, A., L. A. Smith, and E. Suckling (2011), Pattern scaled climate change scenarios: Are these useful for adaptation?, *Grantham Res. Inst. Clim. Change Environ. Working Paper*, *71*, 1–29.

Lopez, A., E. B. Suckling, and L. A. Smith (2013), Robustness of pattern scaled climate change scenarios for adaptation decision support, *Clim. Change*, *122*(4), 555–566, doi:10.1007/s10584-013-1022-y.

Manabe, S., and R. T. Wetherald (1980), Distribution of climate change resulting from an increase in CO_2 content of the atmosphere, *J. Atmos. Sci.*, *37*, 99–118.

May, W. (2012), Assessing the strength of regional changes in near-surface climate associated with a global warming of 2°C, *Clim. Change*, *110*(3–4), 619–644, doi:10.1007/s10584-011-0076-y.

Meinshausen, M., S. C. B. Raper, and T. M. L. Wigley (2011), Emulating coupled atmosphere-ocean and carbon cycle models with a simpler model, MAGICC6: Part I Model description and calibration, *Atmos. Chem. Phys.*, *11*, 1417–1456, doi:10.5194/acp-11-1417-2011.

Mitchell, T. D. (2003), Pattern scaling—An examination of the accuracy of the technique for describing future climates, *Clim. Change*, *60*(3), 217–242.

Moss, R. H., et al. (2010), The next generation of scenarios for climate change research and assessment, *Nature*, *463*, 747–756, doi:10.1038/nature08823.

Santer, B. D., T. M. L. Wigley, M. E. Schlesinger, and J. F. B. Mitchell (1990), Developing climate scenarios from equilibrium GCM results, *Tech. Rep.*, Max–Planck-Institut für Meteorologie, Hamburg, Germany.

Screen, J. A. (2014), Arctic amplification decreases temperature variance in northern mid- to high-latitudes, *Nat. Clim. Change*, *4*, 577–582, doi:10.1038/nclimate2268.

Taylor, K. E., R. J. Stouffer, and G. A. Meehl (2012), An overview of CMIP5 and the experiment design, *Bull. Am. Meteorol. Soc.*, *93*(4), 485–498, doi:10.1175/BAMS-D-11-00094.1.

Tebaldi, C., and J. M. Arblaster (2014), Pattern scaling: Its strengths and limitations, and an update on the latest model simulations, *Clim. Change*, *122*(3), 459–471, doi:10.1007/s10584-013-1032-9.

van Vuuren, D. P., et al. (2011), The representative concentration pathways: An overview, *Clim. Change*, *109*(1–2), 5–31, doi:10.1007/s10584-011-0148-z.

Weaver, A. J., et al. (2012), Stability of the Atlantic meridional overturning circulation: A model intercomparison, *Geophys. Res. Lett.*, *39*, L20709, doi:10.1029/2012GL053763.

Zhang, Y., J. M. Wallace, and D. S. Battisti (1997), ENSO-like interdecadal variability: 1900-93, *J. Clim.*, *10*(5), 1004–1020.